Ömer Üstündağ, Nasim Bakir, Andrey Gumenyuk, Michael Rethmeier

Influence of oscillating magnetic field on the keyhole stability in deep penetration laser beam welding

Üstündağ, Ö., Bakir, N., Gumenyuk, A., & Rethmeier, M. (2021). Influence of oscillating magnetic field on the keyhole stability in deep penetration laser beam welding. Optics & Laser Technology, 135, 106715. https://doi.org/10.1016/j.optlastec.2020.106715

-Short Communication-

Influence of Oscillating Magnetic Field on the Keyhole Stability in Deep Penetration Laser Beam Welding

Ömer Üstündağ[a,*], Nasim Bakir[a], Andrey Gumenyuk[a,b], Michael Rethmeier[c,a,b]

[a]Bundesanstalt für Materialforschung und -prüfung, Berlin, Germany;

[b]Fraunhofer Institute for Production Systems and Design Technology, Berlin, Germany;

[c]Institute of Machine Tools and Factory Management, Technische Universität Berlin, Berlin, Germany

*Corresponding author: Ömer Üstündağ, Phone: +49-30-8104-3150,

E-Mail: oemer.uestuendag@bam.de, Address: Unter den Eichen 87, 12205 Berlin, Germany

Abstract

The stability of the keyhole decreases for deep penetrated high-power laser beam welding. The keyhole tends to collapse with increasing laser power and e.g. keyhole induced porosity can occur. This study deals with the observation of the keyhole during high-power laser beam welding in partial penetration mode by means of a high-speed camera. A butt configuration of 25 mm thick structural steel and transparent quartz glass was used for the experiments. An oscillating magnetic field was applied perpendicular to the welding direction on the root side of the steel plate. The keyhole was highlighted with a coaxial diode laser. It was ascertained that the stability of the keyhole and the weld penetration depth were increased by applying an oscillating magnetic field with an oscillating frequency of 1.2 kHz and a magnetic flux density of 50 mT.

Keywords: laser beam welding; keyhole stability; deep penetration welding; magnetic field; thick-walled steel

1 Introduction

Recent developments in laser technology have brought a new generation of high-power laser systems in the power range between 10 kW to 100 kW to the market. Due to certain technological limitations their application for welding of thick sections is still far from real industrial scale and remains restricted to few cases mostly where the thickness of the parts does not exceed 15 mm for full penetrated welds. Welding results with a 100 kW fibre laser indicates that a weld bead penetration depth in partial penetration mode in the range of approx. 55 mm at welding speeds below 1 m min^{-1} is possible [1]. Several studies regarding high-power laser beam-based welding process show that in the laser power range up to 20 kW the penetration is approx. 1 mm per 1 kW. From 20 kW to 100 kW there is a loss of penetration to approx. 0.5 mm per 1 kW laser beam power [2].

One of the limiting factors and a possible reason for the loss of penetration is the increase of the process instability with the growing laser power applied for the welding process. The process instability in deep penetration welds is favoured mainly by keyhole collapses. The cavity is formed due to the evaporation of the material at a high power density of the laser beam above 10^6 W cm^{-2} and a multiple internal reflection of the beam within the keyhole. The generated keyhole makes the beam reach its bottom and the absorption of the laser beam intensity into the material for a deeper weld penetration depth is increased. The cavity is maintained through the equilibrium between opening forces and closing forces. Forces caused by the surface tension, the hydrostatic pressure and hydrodynamic pressure of the molten pool act to close the keyhole, whereas the opening forces arising from the material ablation and the recoil pressure [3-5]. With an imbalance of the acting forces, the keyhole periodically oscillates through the welding process and the shape and size of the keyhole fluctuates during welding. The higher closing forces can cause a constriction of the keyhole at the bottom, which finally can be separated from the rest of the keyhole and solidifies as a pore, especially at partial penetration. Since the laser beam welding process is known for its high welding speed and resulting solidification rate, the degassing possibility is limited. Several experimental and numerical analyses were performed, where a collapse of the keyhole was detected as a cause to keyhole induced porosity [6-8]. During the collapse of the keyhole a part of the laser beam power is lost for the maintaining of the keyhole, which can also cause a loss of penetration.

Another influencing factor on the keyhole stability and penetration depth is the angle of incidence of the keyhole front. It could be demonstrated that the Fresnel absorptivity is dependent on the wavelength of the laser and the angle of incidence. For solid-state laser with a wavelength of 1064 nm, the Fresnel absorptivity reach its maximum of approx. 40 % at an angle of incidence between 6° to 10° [9]. With a further increase of the keyhole front angle the absorptivity decreases. The absorption depends on the angle of incidence of the beam [10].

To increase the stability of the keyhole during high-power laser beam welding different strategies were used in recent studies. One of these is the application of a reduced ambient pressure or vacuum during laser beam welding. It could be shown that the penetration depth of the keyhole was increased with reduced ambient pressure. The reduction of the ambient pressure leads to a modification of the evaporation pressure inside the keyhole. The weld surface quality and penetration depth were improved with decreasing ambient pressure and the stability of the keyhole was improved [11-14]. Due to process-specific features and challenges such as the necessity of a vacuum chamber for laser beam welding in vacuum, alternative solutions need to be developed, especially for welding of large structures.

With an addition of oxygen to helium shielding gas the stability of the keyhole was increased and the porosity formation was suppressed. The decrease of the surface tension by addition of oxygen was not the reason for a stable keyhole, since the experiments could not be reproduced for a sulphur addition, which is also a surface active element and reduces the surface tension. The main reason for the stabilization of the keyhole was attributed to the formation of CO in the keyhole. The increase in static CO partial pressure leads to a reduction of fluctuations and stabilizing the keyhole [15].

As the state of the art shows, the keyhole behaviour is dependent on many welding parameters and needs to be investigated further, to understand the phenomena inside the keyhole. The dynamics of the keyhole has to be influenced to get a stable keyhole and welding process. First approaches to improve the keyhole stability by external static magnetic field in full penetration laser beam welding of 316L steel was demonstrated in [16], successfully. In previous studies dealing with laser beam based welding by use of an oscillating magnetic field, it could be shown that the melt flow dynamic could be influenced positive to e.g. reduce the porosity of laser beam welded aluminum die casting [17] or to improve the transport of the filler wire elements at hybrid laser arc welding through formation of a vortex within the melt pool [18]. This study deals with the influence of an external oscillating magnetic field during high-power laser beam welding on the keyhole stability and on the laser beam incident angle.

2 Experimental Setup

The high-power Yb:YAG thin disk laser TruDisk 16002 with a maximum output power of 16 kW was used as the laser beam source. The emission wavelength and beam parameter product were 1030 nm and 8 mm x mrad, respectively. The laser radiation was transmitted through an optical fibre with a core diameter of 200 µm. A laser-processing head YW52 has been selected, which provides a magnification of 2.1 so that the laser beam can be focused into a spot with a diameter of 420 µm. To detect the keyhole during high-power laser beam welding a special setup was necessary. A butt configuration of 25 mm thick structural steel plate (S355J2) and quartz glass was conducted. This experimental setup has also used from several researchers to study the keyhole behavior during the laser welding such as in [19]. A diode laser with a wavelength of 808 nm and a max. output power of 100 W was mounted onto the optical head of the laser and introduced coaxially to the beam axis of the welding laser to illuminate the keyhole. The beam of the diode laser propagates inside the keyhole and illuminates it. Side views of the keyhole were taken with help of a highspeed camera Fastcam 1024PCI and interference band-pass filter at 808 nm and band width of 20 nm. The frame rate was 3600 fps. An oscillating magnetic field generated by an AC electromagnet was applied to the root side of the weld specimen, where the magnetic field was perpendicular and induced electric current parallel or antiparallel to the welding direction. The schematic representation of the experimental setup is shown in Figure 1.

The welding experiments were performed using 16 kW laser beam power at a welding speed of 1 m min^{-1}. The focal position of the laser beam was set to -5 mm relative to the workpiece surface. The magnet was positioned 2 mm below the weld specimen and operated with an oscillating frequency of 1150 Hz, an AC power of 770 W and a magnetic flux density of 50 mT. This magnet parameters were chosen from previous study for welding the same materials thicknesses [20]. The oscillating frequency has an influence on the skin layer depth. As the frequency increases, the current flow moves to the surface, resulting in less skin depth. The calculation of the skin layer depth is as follows [21]:

$$\delta = \sqrt{\frac{1}{\pi f \sigma \mu}}$$

where δ is the skin layer depth, f is the oscillating frequency, σ is the electrical conductivity and μ is the permeability. The electromagnetic pressure (p_{EM}) which is acting upwards is influenced by the magnetic flux density (B) and can be calculated as follows [22]:

$$p_{EM} = \frac{B^{2}}{2\mu_0}$$

The impact of the magnet parameters such as the frequency and the magnet power are not a part of the study therefore were kept constant for all experiments. The aim is to investigate the influence of the magnetic flied during deep penetration welding on the keyhole stability.

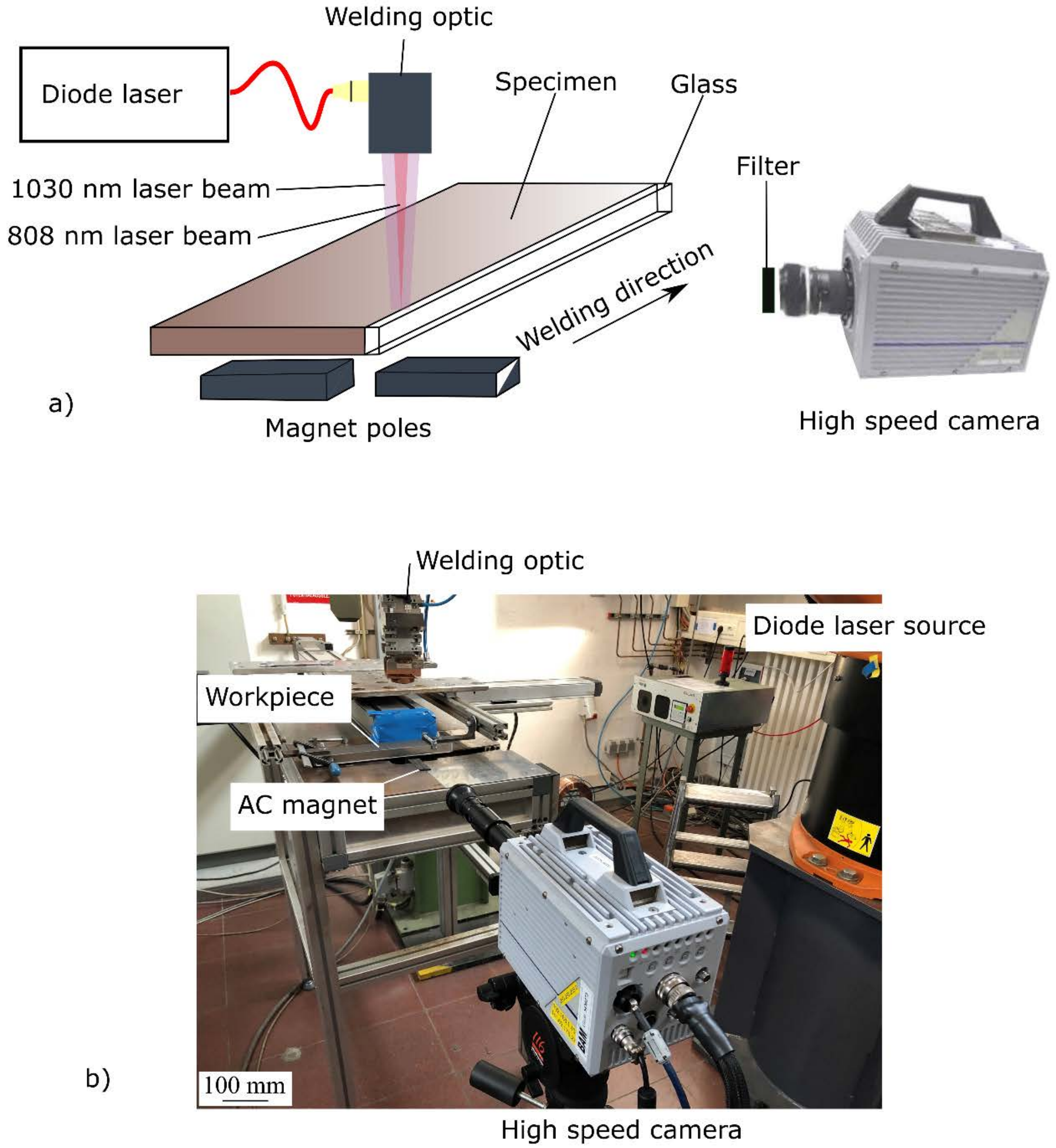

Figure 1. (a) Schematic representation of the experimental setup and (b) experimental setup

3 Results and discussion

Thanks to the additional laser beam inserted into the main laser beam path, and the application of the appropriate interference filter in front of the camera lens, the recorded videos represents only the keyhole surfaces through the quartz glass as a result of the multiple laser beam reflections on its surface. Two different keyhole types can be identified based on the high-speed recordings. Figure 2 shows four sequences for the longitudinal profile of the keyhole with application of the magnetic field (a) and without it (b). Two significant differences can be clearly identified, firstly the keyhole shape and secondly the keyhole depth. In the case where the magnet is applied, the keyhole profiles take conical shape, is much deeper and has a pointed end in contrast to the case where the magnetic field is not applied, where the keyhole showed rounded root and almost take a cylindrical form.

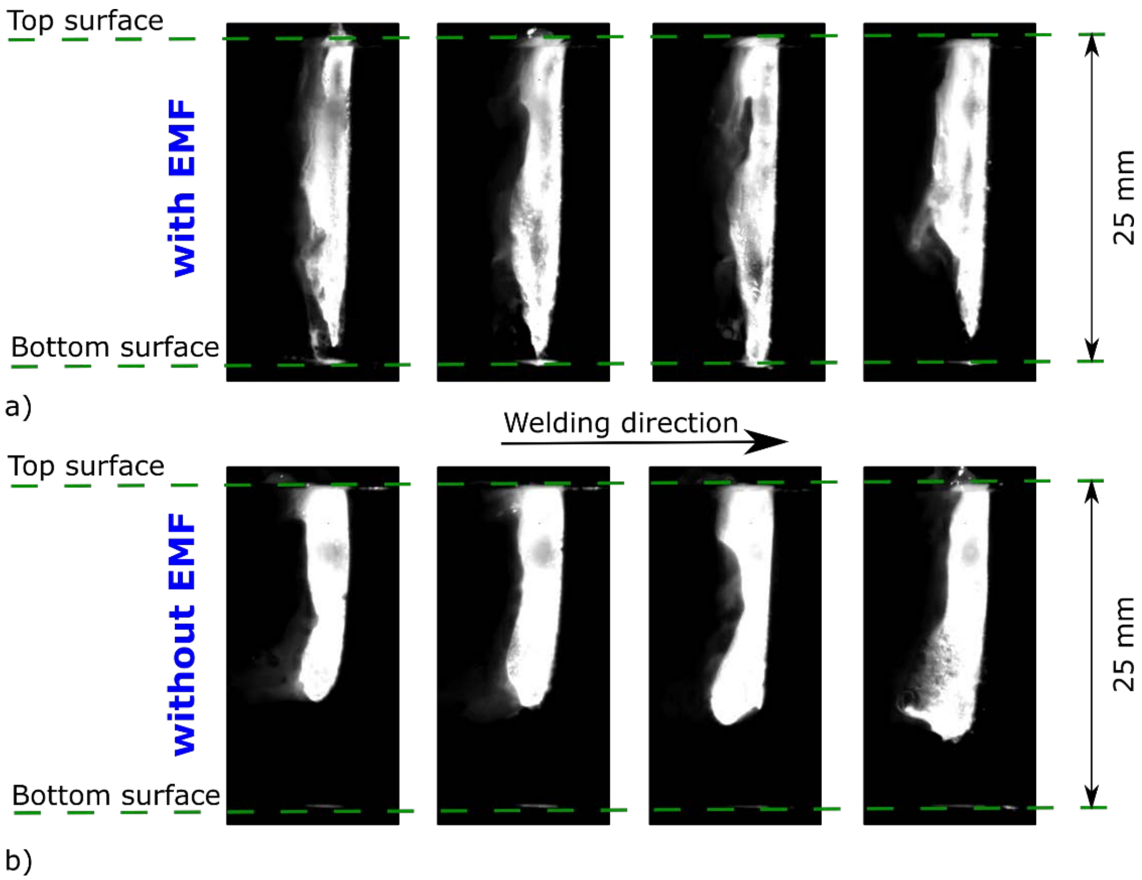

Figure 2. (a) Observed longitudinal profile of the keyhole during the welding under electromagnetic field (EMF) for four sequences; (b) without EMF

For a better evaluation of the keyhole profile and the weld penetration, the image processing technique (edge detection) using a Matlab routine for finding the boundaries of the keyhole for all video sequences was employed. Additionally, two cross-sections were taken in two places to determine the welding depth. Figure 3 (a) and (b) show the comparison between the cross-sections, the high-speed images and the estimated keyhole profiles with and without applying the EMF, respectively. Very good matching can be for this comparison noted.

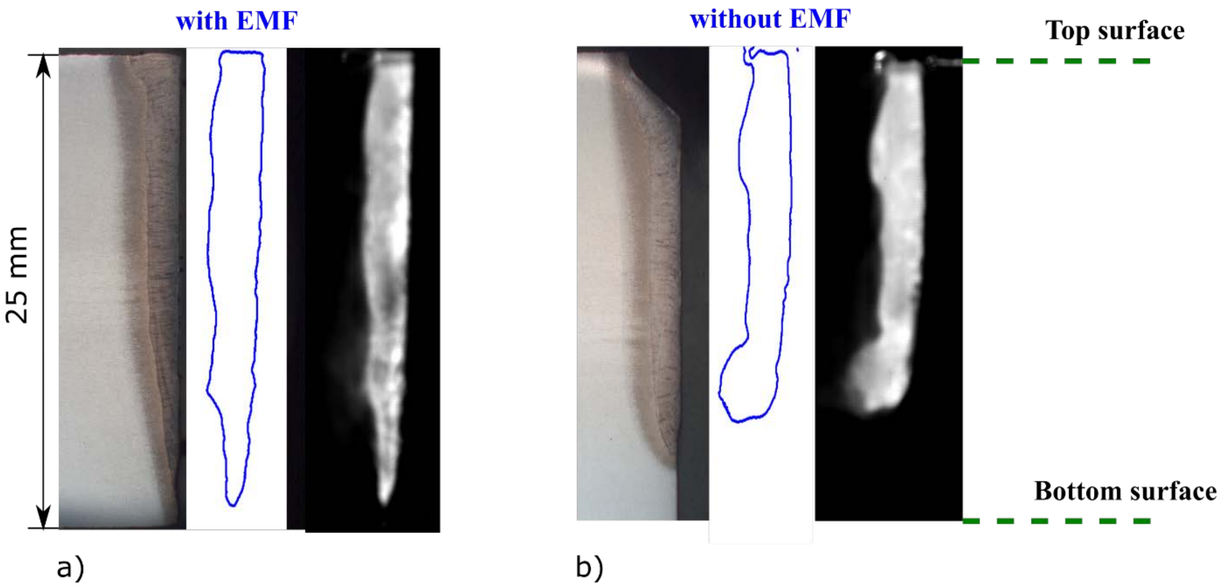

Figure 3. Comparison between the estimated keyhole and the corresponding cross-section (a) with EMF and (b) without EMF

Figure 4 (a) shows side-by-side plotted longitudinal profile of the keyhole over the time. The red dashed line represents the time of shutting down of the EMF. Figure 4 (b) shows the fused material traces on the quartz glass welding and Figure 4 (c) the overlapping of the estimated longitudinal welding profile on the glass. Very good concordance can be established between the experiments and the estimation technique. The difference in welding depth can be clearly recognized. At the beginning, almost continuous keyhole through the specimen thickness can be detected and after turning off the EMF the keyhole depth decreases and fluctuates between 18 mm and 15 mm in a weld length of approx. 50 mm. After that time the penetration depth is constant at 15 mm.

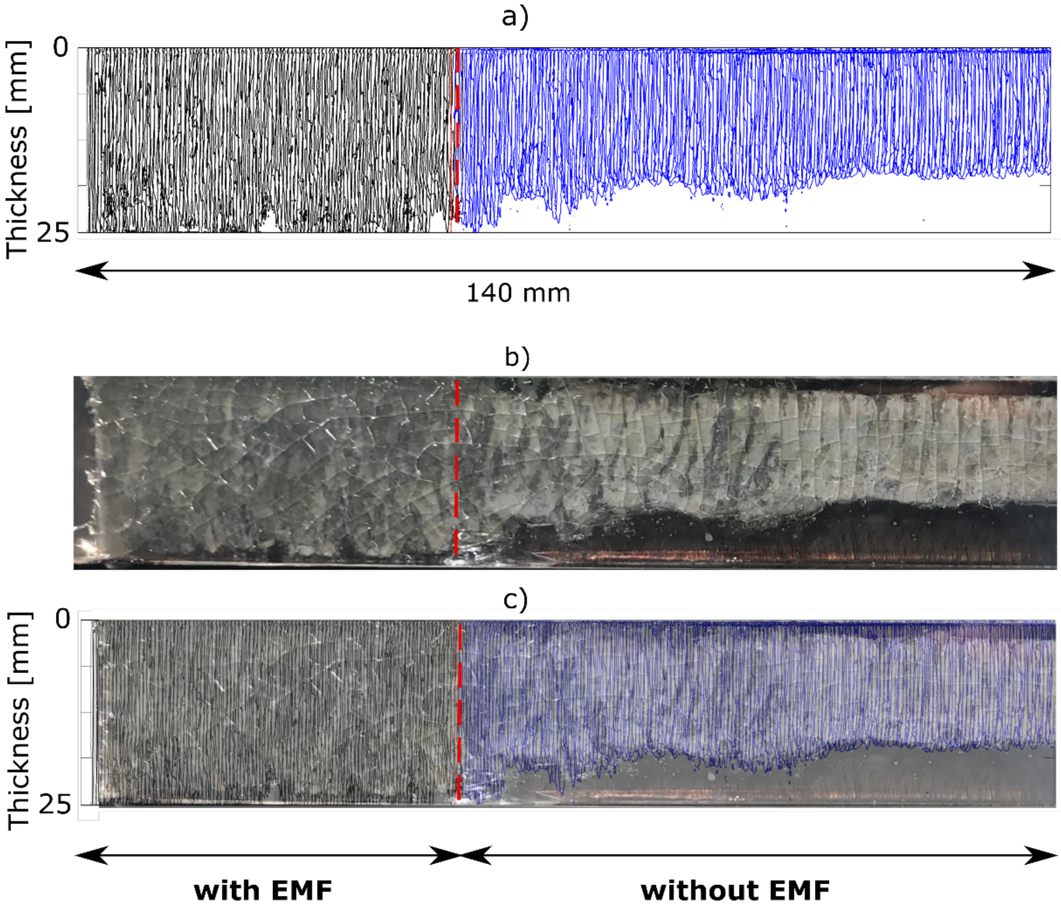

Figure 4. (a) Side-by-side plotted longitudinal profile of the keyhole over the specimen length, (b) side view of the quartz glass after the welding, (c) the estimated keyhole profiles overlapped on the glass

Another phenomenon was also observed. The incidence angle α between the keyhole front and laser beam axis, is significantly higher in the case without EMF, as shown in Figure 5. The incidence angle has a major impact on the absorption coefficient [23]. This, together with other factors, plays an important role on the welding depth. The incidence angle was measured on different high-speed images. In the case of EMF and without EMF the inclination angle was 8.2° ± 1.6° and 16.4° ± 1.1° respectively. The reduction of the incidence angle has already been observed by [16]. By the application of an external magnetic field, the incidence angle was reduced and thus the degree of absorption of laser beam increased.

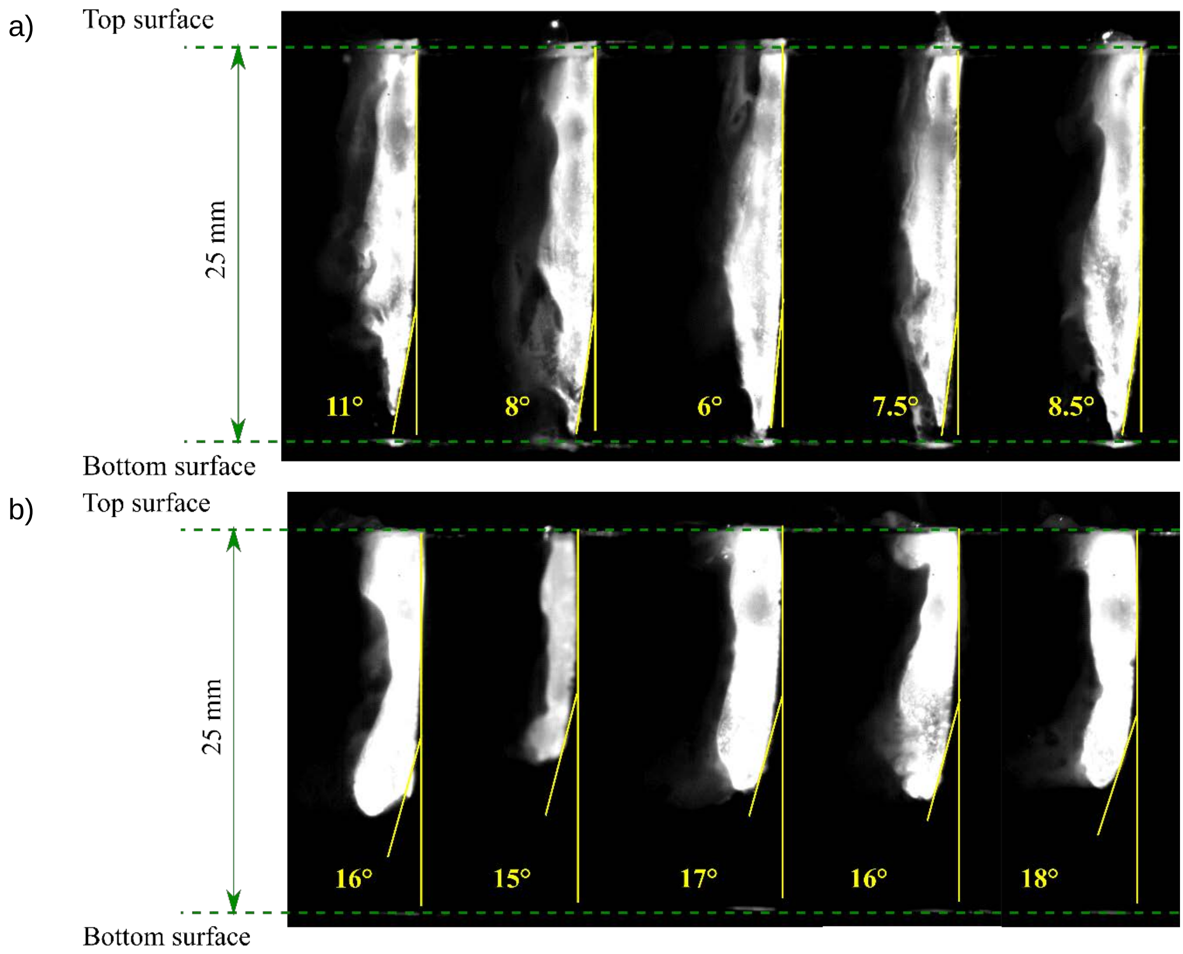

Figure 5. Comparison of the incidence angle α of the keyhole front between (a) under EMF and (b) without EMF

It can be assumed that the magnetic forces acting on the melted material have a direct influence on the flows in the keyhole surrounding, which helps to keep the keyhole open.

The keyhole having a cylindrical shape in the first approximation does not experience any resistance in the flow of a surrounding liquid due to boundary conditions associated with the sliding of the liquid along the interphase boundary, similar to the case of a solid sphere surrounded by a flow of an ideal liquid in contrast to the case of a solid sphere surrounded by a flow of a viscous liquid, where the viscous boundary layer forms in the near of the solid body surface. In the latter case, the drag force can be calculated using the known Stokes formula:

$$F_S = 6\,\pi\,\rho\nu\,r\,u$$

where ν is the kinematic viscosity, r is the radius of the sphere, u is the velocity and ρ is the mass density of the fluid.

Under the conditions of the action of an electromagnetic field and, in particular, the flow of an induced electric current, there is an additional resistance force associated with the action of the rotary component of electromagnetic forces.

Due to the fact, that the keyhole is a vapor filled capillary and the electrical conductivity is very low, the course of the electric current is redirected and concentrated at the keyhole side wall. The Lorentz force, which is always perpendicular to the magnetic field lines and to the direction of the movement of the electric charge (right-hand rule) consists of two components a potential and a rotatory component (as rot F_L = rot [B x j] ≠0 due to the inhomogeneous course of the electric current, which becomes not orthogonal to the magnetic field lines). A scheme of the magnetic and electric field during laser beam welding of steel/quartz glass configuration with EMF is shown in Figure 6. The order of magnitude of the resistance force can be calculated according to the formulas given in the work [24] with an accuracy to correcting coefficients in case of nonconductive sphere:

$$F_t = F_S + F_{EM} = 6\,\pi\rho\nu\, ru\left[1 + \frac{ru}{8\nu}\left(3 + \frac{\mu_0 j^2 r^2}{\rho u^2}\right)\right]$$

where μ_0 is the magnetic permeability in a classical vacuum and j is the electric current density. Based on characteristic values for laser beam welding with parallel influence of induced electromagnetic fields, it can be hundreds of times higher than the resistance forces calculated on the basis of the Stokes formula for body movement in a flow of viscous fluid. The rotary component is similar to a friction force and leads to significant slowing down the flow velocity in the vicinity of keyhole surface. Due to the action of the viscous electromagnetic forces, the decrease of the hydrodynamic pressure, which is proportional to the square of the local melt velocity at the keyhole surface, takes place. This contributes to achieving a force balance at the keyhole surface corresponding to the lower evaporation temperature and therefore much lower vapor recoil pressure. According to [25] the magnetic flux density and the generated Lorentz force cause a reduction of the melt displacement within the molten pool, suggesting that the homogeneity of the heat distribution in the thickness direction increased and the utilization of the laser energy was improved by the magnetic field.

In other words, the EMF could have an important influence on the stabilization of the keyhole during the deep laser beam welding process, like the case of laser beam welding under reduced pressure.

This of course helps the laser beam to melt more material in the keyhole root instead of using laser power to open the keyhole again in the case of a fluctuating keyhole. That is probably the main reason for the difference between the welding depths with and without using magnet technology.

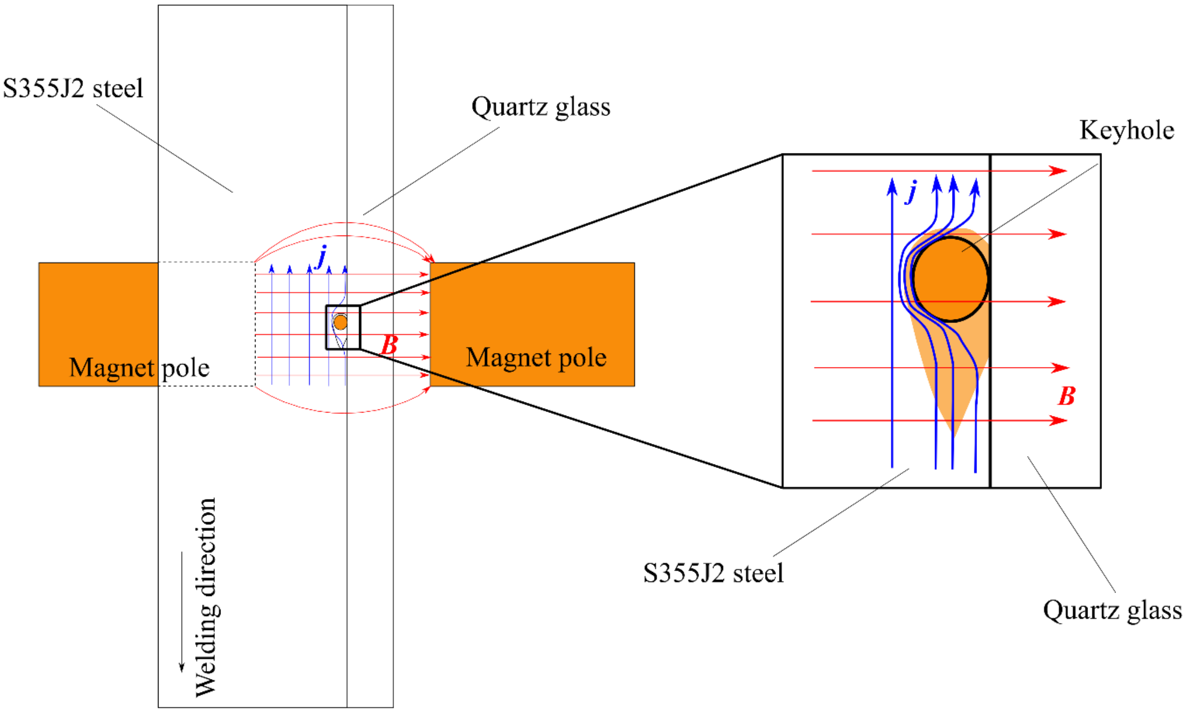

Figure 6. Scheme of the magnetic and electric field during laser beam welding of steel/quartz glass configuration with EMF

4 Conclusion

In this short communication paper, the authors would like to draw the attention to a very interesting observations of keyhole behaviour by using the EMF and its influence on the welding depth. A high-speed camera was employed to record the keyhole profile longitudinally through a quartz glass prepared in butt configuration with a steel plate. Significant differences were found by applying the EMF compared to the case without the EMF. Firstly, the keyhole was deeper in the case of applying the EMF. Secondly, the keyhole profiles in the case without EMF, show higher incidence angles between the keyhole front and laser beam axis

References

[1] Katayama, S., Mizutani, M., Kawahito, Y., Ito, S., & Sumimori, D. (2015). Fundamental research of 100 kW fiber laser welding technology. In Proceedings of Lasers in Manufacturing (LiM), World of Photonics Congress, Munich.

[2] Nielsen, S. E. (2015). High power laser hybrid welding–challenges and perspectives. Physics Procedia, 78, 24-34.

[3] Katayama, S. ed., (2013). Handbook of laser welding technologies. Elsevier.

[4] Kannatey-Asibu Jr, E., (2009). Principles of laser materials processing (Vol. 4). John Wiley & Sons.

[5] Ion, J., (2005). Laser processing of engineering materials: principles, procedure and industrial application. Elsevier.

[6] Courtois, M., Carin, M., Le Masson, P., Gaied, S., & Balabane, M. (2014). A complete model of keyhole and melt pool dynamics to analyze instabilities and collapse during laser welding. Journal of Laser Applications, 26, 042001.

[7] Huang, L., Hua, X., Wu, D., & Ye, Y. (2019). Role of welding speed on keyhole-induced porosity formation based on experimental and numerical study in fiber laser welding of Al alloy. The International Journal of Advanced Manufacturing Technology, 103, 913-925.

[8] Matsunawa, A., Mizutani, M. Katayama, S. & Seto, N. (2003). Porosity formation mechanism and its prevention in laser welding. Welding International, 17, 431-437.

[9] Kaplan, A. F. H. (2012). Absorptivity modulation on wavy molten steel surfaces: The influence of laser wavelength and angle of incidence. Applied Physics Letters, 101(15), 151605.

[10] Bergström, D. (2008). The absorption of laser light by rough metal surfaces. PhD Thesis, Luleå University of Technology, Sweden.

[11] Jiang, M., Chen, X., Chen, Y. & Tao, W. (2019). Increasing keyhole stability of fiber laser welding under reduced ambient pressure. Journal of Materials Processing Technology, 268, 213-222.

[12] Jiang, M., Tao, W., & Chen, Y. (2017). Laser welding under vacuum: a review. Applied Sciences, 7(9), 909.

[13] Katayama, S., Kobayashi, Y., Mizutani, M., & Matsunawa, A. (2001). Effect of vacuum on penetration and defects in laser welding. Journal of Laser Applications, 13(5), 187-192.

[14] Reisgen, U., Olschok, S., Jakobs, S., & Turner, C. (2016). Laser beam welding under vacuum of high grade materials. Welding in the World, 60(3), 403-413.

[15] Zhao, L., Tsukamoto, S., Arakane, G., & Sugino, T. (2014). Prevention of porosity by oxygen addition in fibre laser and fibre laser–GMA hybrid welding. Science and Technology of Welding and Joining, 19(2), 91-97.

[16] Li, M., Xu, J., Huang, Y., & Rong, Y. (2018). Improving keyhole stability by external magnetic field in full penetration laser welding. JOM, 70(7), 1261-1266.

[17] Fritzsche, A., Hilgenberg, K., Teichmann, F., Pries, H., Dilger, K., & Rethmeier, M. (2018). Improved degassing in laser beam welding of aluminum die casting by an electromagnetic field. Journal of Materials Processing Technology, 253, 51-56.

[18] Üstündağ, Ö., Avilov, V., Gumenyuk, A., & Rethmeier, M. (2019). Improvement of filler wire dilution using external oscillating magnetic field at full penetration hybrid laser-arc welding of thick materials. Metals, 9(5), 594.

[19] Zhang, Y., Lin, Q., Yin, X., Li, S. & Deng, J. (2018). Experimental research on the dynamic behaviors of the keyhole and molten pool in laser deep-penetration welding. Journal of Physics D: Applied Physics, 51(14), p.145602.

[20] Üstündağ, Ö., Fritzsche, A., Avilov, V., Gumenyuk, A. & Rethmeier, M. (2018). Hybrid laser-arc welding of thick-walled ferromagnetic steels with electromagnetic weld pool support. Welding in the World, 62(4), pp.767-774.

[21] Landau, L.D. & Lifshits, E.M. (1982). Theoretical Physics, Vol. 8: Electrodynamics of Continuous Media.

[22] Avilov, V., Fritzsche, A., Bachmann, M., Gumenyuk, A. & Rethmeier, M. (2016). Full penetration laser beam welding of thick duplex steel plates with electromagnetic weld pool support. Journal of Laser Applications, 28(2), p.022420.

[23] Zou, J., Ha, N., Xiao, R., Wu, Q., & Zhang, Q. (2017). Interaction between the laser beam and keyhole wall during high power fiber laser keyhole welding. Optics express, 25(15), 17650-17656.

[24] Chow, C. Y., & Halat, J. A. (1969). Drag of a Sphere of Arbitrary Conductivity in a Current-Carrying Fluid. The Physics of Fluids, 12(11), 2317-2322.

[25] Xu, J., Rong, Y. and Huang, Y. (2019). Magnetic-Field-Induced Partial-to-Full Penetration Evolution and Its Mechanism During Laser Welding. JOM, 71(7), pp.2296-2302.